Environmental Science and Pollution Research (2023) 30:42563–42574
https://doi.org/10.1007/s11356-022-18996-4

RECENT TRENDS ON SUSTAINABLE AGRICULTURE THROUGH ENVIRONMENTAL FRIENDLY PESTICIDES: AN ECOLOGICAL CONSERVATION APPROACH

Biosynthesis of copper oxide nanoparticles using *Rubia cordifolia* bark extract: characterization, antibacterial, antioxidant, larvicidal and photocatalytic activities

Annadurai Vinothkanna[1,2] · Krishnamurthy Mathivanan[3] · Sivapunniyam Ananth[4] · Yongkun Ma[1] · Soundarapandian Sekar[2]

Received: 17 November 2021 / Accepted: 27 January 2022 / Published online: 17 February 2022

Abstract

Rubia cordifolia represents the pivotal plant resource belonging to traditional Chinese medicine and Indian Ayurveda. The present study aims to synthesize biocompatible copper oxide nanoparticles (CuONPs) using *R. cordifolia* bark extracts, characterize the incumbent chemical transitions, and explore their biomedical and environmental applications. The absorbance peak between 250 and 300 nm clearly demonstrates the formation of CuONPs in the UV–visible spectrum. Fourier transform infrared spectroscopy results showed the presence of functional groups essential for copper ion reduction. Field emission scanning electron microscopy (FE-SEM) and dynamic light scattering analysis revealed that the CuONPs are spherical-shaped with a mean particle size of 50.72 nm. Additionally, the zeta potential demonstrates its robustness at 11.2 mV. X-ray diffraction pattern showed mixed phases (Cu, Cu_2O, and CuO) of cubic monoclinic crystalline nature. CuONPs exhibited noticeable antibacterial activity against Gram-negative (*Escherichia coli* and *Pseudomonas aeruginosa*) and Gram-positive (*Staphylococcus aureus* and *Bacillus cereus*) pathogenic bacteria. Bacterial cell damages were affirmed through FE-SEM imaging when treated with CuONPs. Further, CuONPs demonstrated considerable antioxidant activities by quenching free radicals such as DPPH (60.75%), ABTs (70.88%), nitric oxide (65.48%) and reducing power (71.44%) in a dose-dependent way. CuONPs showed significant larvicidal activity against *Aedes aegypti* (65 ± 8.66%), *Anopheles stephensi* (80 ± 13.69%), and *Culex quinquefasciatus* (72 ± 13.04%) mosquito larvae. The photocatalytic activity of the CuONPs demonstrates the methylene blue (81.84%) and crystal violet (64.0%) dye degradation potentials, indicating the environmental bioremediation efficacy. Hence the present study is the first report in accounting for the versatile applications of the phyto-CuONPs. Moreover, the green synthesis of CuONPS has future applications in designing the drug for life-threatening diseases and various environmental issues.

Keywords *Rubia cordifolia* · CuONPs · Antioxidant potential · Antibacterial · Larvicidal · Photocatalysis

Introduction

Rubia cordifolia belonging to the Rubiaceae family are predominantly present in hilly regions like the Himalayas with antibacterial, anti-inflammatory, antioxidant, and

Responsible Editor: Sami Rtimi

✉ Yongkun Ma
mayongkun@ujs.edu.cn

✉ Soundarapandian Sekar
sekarbiotech@yahoo.com

[1] School of Food and Biological Engineering, Jiangsu University, 301 Xuefu Road, Zhenjiang 212013, People's Republic of China

[2] Department of Biotechnology, Bharathidasan University, Tiruchirappalli 620 024, Tamil Nadu, India

[3] School of Minerals Processing and Bioengineering, Central South University, Changsha, Hunan 410083, People's Republic of China

[4] Sivan Bioscience Research and Training Laboratory, Kumbakonam, Tamil Nadu, India

anticonvulsion potentials (Deshkar et al. 2008; Gong et al. 2017). Further antihemolytic properties of the *Rubia* species have been established in traditional Chinese medicine in curing various blood circulation complications like dysmenorrhea and blood stasis (Chen et al. 2021; Gong et al. 2017; Hu et al. 2020). Nevertheless, the *R. cordifolia* shows promising benefits in Ayurveda against various circulatory, urinary, and integumentary complications (Deshkar et al. 2008; Meena 2015). The plant also called munjeet/Manjeet (*R. cordifolia* L.) remains a prominent dye (red, scarlet, brown, and mauve) in the cotton and woolen fabric industries of the Asian subcontinent (Deshkar et al. 2008; Gleba et al. 2016). Natural dye extraction procedures employing *R. cordifolia* roots henna extracts using wool as substrate showed antifungal properties (Yusuf et al. 2017, 2015). *Rubia cordifolia* (Manjishtha) barks have been used in the preparation of many Ayurvedic and Siddha polyherbal-based products which have several therapeutic applications (Sekar and Mariappan 2010). Barks generally contain a wide spectrum of secondary metabolites (especially polyphenols, alkaloids, flavonoids, lignans, terpenes, and taxanes) with biological activity that includes antioxidant, antimicrobial, and anticancer properties (Burlacu and Tanase 2021). Biosynthesis of nanoparticles using plant barks extracts is investigated by eco-friendly and cost-effective approach. CuONPs using bark extracts of cinnamon and *Syzygium alternifolium* (Wt.) showed antimicrobial, anticancer, and dye degradation potential (Sarwar et al. 2021; Yugandhar et al. 2017). Until date copper nanoparticle synthesis from *R. cordifolia* has not been documented for influential roles in dye degradation and antibacterial activities collectively. The present research report coerces the existing versatile applications of *R. cordifolia* in biosynthesis of copper nanoparticles (CuONPs) for eco-friendly bioremediation and biodegradation perspectives together with bioactive potentials. Similar works employing green synthesis of CuONPs from *Allium sativum* extract showed antimicrobial, antioxidant, and larvicidal activities (Velsankar et al. 2020). Further, copper oxide nanoparticles synthesized based on cost-effective green chemistry approaches revealed antibacterial activity and dye degradation potential by photocatalysis (Sathiyavimal et al. 2018, 2021; Vasantharaj et al. 2019). In another study, silver nanoparticles were synthesized using the aqueous extracts of *R. cordifolia* depicted antibacterial, antibiofilm, and hemolytic potentials effectively (Mariswamy et al. 2021). Similarly, eco-friendly synthesis of zinc oxide nanoparticles mediated via *R. cordifolia* showed antioxidant and photocatalytic activity (Negi 2018). Further, eco-friendly and cost-effective synthesis of copper and zinc oxide nanoparticles showed larvicidal potential against *Aedes aegypti* and *Culex tritaeniorhynchus* and prevent mosquito-borne diseases such as dengue and Japanese encephalitis (Velsankar et al. 2020; Vinotha et al. 2020).

Limited studies in establishing the *R. cordifolia* CuONPs affirming Ayurvedic authentication in traditional use with eco-friendly dye degradation prospects need to be unraveled. As a result, an attempt was made to elucidate the most important applications of R. *cordifolia* CuONPs. Standard techniques in deciphering the optimal characterization of the synthesized CuONPs and potential radical scavenging activities were derived. Combinatorial verification of antioxidant potentials will establish the anticancer properties of CuONPs through preliminary validation from the present study. Antibacterial activities towards Gram-negative and Gram-positive bacteria comprising the normally encountered environmental contamination are incumbent for bioactivities of the CuONPs. Further, green synthesized cost-effective and biodegradability CuONPs control mosquito larval growth and prevent principal mosquito-borne diseases such as dengue, malaria, and Japanese encephalitis. Photocatalytic activities were performed for advocating the basis of the *R. cordifolia* CuONPs as eco-friendly component combating dye degradation effectively.

Materials and methods

Plant material and preparation of bark extract

Rubia cordifolia barks were collected from locally available market, Tiruchirappalli, Tamil Nadu, India. It was shadow dried and thoroughly washed under running tap water to remove any possible impurities. Briefly, 10 g of *R. cordifolia* barks was chopped into small pieces boiled in 100 mL of double-distilled water for 10 min. Subsequently the extract was cooled to room temperature and filtered using Buchner funnel and Whatman No. 1 filter paper. Finally, the purified aqueous solution/extract was used for further study.

Biosynthesis of copper oxide nanoparticles

The biosynthesis of copper oxide nanoparticles was performed according to Sathiyavimal et al. (2018). Precisely, 10 mL of 10% bark extract-aqueous solution was added with 90 mL of 1 mM aqueous copper sulfate ($CUSO_4$) solution, under continuous stirring at 100 °C for 2 h which aids in copper ions reduction. After that, the color suspension changed gradually from light brown to deep dark brown, indicating the formation of CuONPs. Further, the CuONPs solution was purified using sterile deionized water through repeated centrifugation at 10,000 rpm for 10 min, to ensure a better separation of free entities from the metal nanoparticles. Then the precipitated CuONPs solution was dried at 90 °C for 8 h. Finally, the CuONPs powder was collected and used for further research.

Physical characterization of copper oxide nanoparticles (CuONPs)

UV–visible and Fourier transform infrared (FT-IR) spectroscopy analysis

Biosynthesis of CuONPs was primarily characterized utilizing a UV–visible spectrophotometer (Jasco V-650, Japan) set to the range of wavelength within 300–800 nm (Sankar et al. 2014). FT-IR (JASCO FT-IR 4700) was used to decipher the functional groups present in the synthesized CuONPs. Precisely, a disc composed of hydraulic pressure was prepared to employ the addition of 1 mg of CuONPs with 10 mg of potassium bromide (KBr) pellets after grinding well. The spectral range in the 4000–400^{-1} nm was cataloged using FT-IR spectroscopy (Sankar et al. 2014).

X-ray diffraction (XRD) analysis

X'Pert Pro X-ray diffractometer was used to interpret the XRD patterns to establish the CuONPs encapsulated in the drop-coated films. The parameters used are voltage, 40 kv, and current, 30 mA. The nanoparticles size (L) was estimated using Debye–Scherrer's equation utilizing PAN analytical X pert PRO model along with Cu Kα radiation (Singh et al. 2019).

$$L = 0.9\lambda/\beta\cosh\theta$$

where λ is wavelength of the X-ray; β is full width and half maximum h of the X-ray, and θ is Bragg's angle.

Field emission scanning electron microscopic (FE-SEM) analysis with EDAX

FE-SEM (FE-SEM, Carl Zeiss – Σigma model, Germany) was used to analyze the morphological changes of the *R. cordifolia* synthesized CuONPs with a 10 kV accelerating voltage. Briefly, 5 mg of CuONPs is positioned in a double-sided metal stub and added 10 nm gold (Au) thickness for obtaining clear micrographs. Further affirmation of the characterized nanoparticles was subjected to dynamic light scattering (DLS) and zeta potentials for determining the particle sizes of the CuONPs (Vasantharaj et al. 2019).

Antibacterial activity of R. cordifolia CuONPs

Bacterial pathogens

The Gram-negative (*Escherichia coli* MTCC 1610 and *Pseudomonas aeruginosa* MTCC 1953) and Gram-positive (*Staphylococcus aureus* MTCC 96 and *Bacillus cereus*) bacterial pathogens were procured from Microbial Type Culture Collection (MTCC), Institute of Microbial Technology (IMTECH), Chandigarh, India.

Agar well diffusion method

Agar well diffusion method was utilized for estimating the antibacterial activity of the CuONPs (Vasantharaj et al. 2019). The pathogenic microorganisms were sub-cultured in Luria Bertani (LB) broth and incubated overnight at 37 °C overnight for optimal growth conditions. The bacterial cultures were attuned with 0.5 McFarland standards (1×10^8 CFU/mL) which were spread on Mueller Hinton agar plates. CuONPs (100 µL) were added to the well on the agar plates and incubated for 24 h at 37 °C. Zone of inhibition (diameter) was calculated, and the experiment was accomplished in triplicates.

SEM analysis of antibacterial activity

Briefly, 100 µL of log-phase bacterial cultures (10^8CFU/mL) treated with CuONPs (500 µg/mL) at 37 °C for 3 h of incubation. Further, it was centrifuged at 3000 × *g* for 10 min. The harvested pellets were collected and resuspended with 10 mL of 1 × phosphate buffered saline (PBS) solution (pH 7.4). Then, the collected pellets were washed thrice with PBS buffer to eliminate residual media. Further, the pellets were re-suspended in 500 µL of glutaraldehyde solution (2.5%) in 0.1 M Tris-buffered saline (TBS) and allowed to stand for 30 min at 37 °C. After that, the pellets were washed and re-suspended in 0.1 M TBS. Then, 50 µL of the bacterial suspension was added onto a poly-L-lysine coated coverslip. The samples were air-dried using absolute ethanol and sputter coated with a double-sided metal stub with a 10 nm gold (Au) thickness to obtain clear micrographs. Finally, the samples were observed using FE-SEM (Carl Zeiss – Σigma model, Germany) and recorded images.

In vitro *antioxidant assay*

2,2-diphenyl-1-picrylhydrazyl (DPPH) scavenging activity

The antioxidant activity of CuONPs was evaluated using DPPH assay to neutralize free radicals (Vinothkanna and Sekar 2018). Briefly, 1 mL of DPPH (0.1 mM) in ethanol was added to the various concentrations of 10, 20, 40, 60, 80, and 100 µg/mL CuONPs in a test tube. These mixtures were shaken well and kept in the dark for 30 min. The absorbance was measured using a UV–Vis spectrophotometer (JASCO V-650, Japan) at 517 nm. L-ascorbic acid was used as a positive standard. Higher scavenging activity was corroborated by low absorbance values. Scavenging capability or the inhibition are calculated using:

$$\text{Inhibition } (\%) = \frac{A_C - A_S}{A_C} \times 100$$

where *Ac* = control and *As* = sample.

2,2'-azino-bis (3-ethylbenzothiazoline-6-sulphonic acid (ABTS) radical scavenging assay

The antioxidant activity of CuONPS was determined using ABTS radical scavenging assay by decolorization (Vinothkanna and Sekar 2018). Briefly, 7 mM ABTS and 2.45 mM of potassium persulfate were added in equal amounts and stored in the dark at a suitable temperature for the generation of cation radical. Dilutions of the solution prepared are optimized with double distilled water to set 0.700 absorbance values at 734 nm wavelength. Equal volume of CuONPs with 10, 20, 40, 60, 80, and 100 µg/mL concentrations (w/v) was vortexed and after 6-min incubation preceded measurements. The experiment was carried out in triplicates, and scavenging capabilities were calculated using ABTs as standard similar to DPPH assay based on A_{734nm} values.

Nitric oxide (NO) radical scavenging assay

The nitric oxide radical scavenging activity of CuONPs was evaluated by Griess-llosvoy reaction (Vinothkanna and Sekar 2018). Briefly, 0.5 mL of sodium nitroprusside (5 mM) in phosphate-buffered saline (PBS) (pH 7.4) and 1 mL of CuONPs at different concentration (10, 20, 40, 60, 80, and 100 µg/mL) were mixed thoroughly. This reaction mixture was incubated at 25 °C for 150 min. After the incubation period, nitrite produced from sodium nitroprusside was measured by adding Griess reagent (1% sulphanilamide, 5% phosphoric acid, and 0.1% 1-naphthalene diamine dihydrochloride in water). The absorbance was immediately read at 570 nm using a UV–Vis spectrophotometer. The nitric oxide scavenging effect was calculated by comparing the absorbance values of control and positive standard (L-ascorbic acid).

Reducing power assay

Reducing power activity of the CuONPs was determined (Vinothkanna and Sekar 2018) with minor modifications. Different dilutions (w/v) (10, 20, 40, 60, 80, and 100 µg/mL) of CuONPs were used. The reaction consists of a 1 mL sample, phosphate buffer (2.5 mL in 0.2 M, pH 6.6), and potassium ferricyanide (2.5 mL in 1%) and subjected to water bath incubation for 20 min at 50 °C. To inhibit the reaction, TCA was used (2.5 mL in 10%). Finally, the tubes were centrifuged (3000 × *g*) for 10 min. From this supernatant, 2.5 mL was mixed with an equal volume of distilled water and ferric chloride (0.1 mL in 0.1% w/v) followed by 10-min incubation. A_{700nm} was measured with reference to the L-ascorbic acid standard. Higher absorbance values denote higher reducing power.

Larvicidal activity of CuONPs

Collection of eggs and larval rearing

Mosquito eggs were procured from the center for research in medical entomology, Madurai, Tamil Nadu, India, and reared in the laboratory under optimal conditions (temperature 27 ± 2 °C, relative humidity: 75–80%, 14 L:10 D photoperiod). The eggs were hatch in the six enamel trays (18 × 13 × 4 cm) containing 500 mL of tap water. After hatching, the larvae were fed with yeast and dry biscuits in a 3:1 ratio. Feeding was continued until larvae transformed into pupae.

Larvicidal bioassay of CuONPs

The larvicidal bioassay of *Aedes aegypti*, *Anopheles stephensi*, and *Culex quinquefasciatus* larvae (IV instar) was carried out with different concentrations (10, 20, 30, 40, and 50 ppm) of CuONPs mediated by *R. cordifolia* bark extract. The larvae were introduced into a beaker containing 249 mL of water and 1 mL of CuONPs. Briefly, 20 larvae in five replicates were used for each dose tested. Mortality rates of larvae was recorded after 24 h post-treatment and expressed in percentage. The control mortality was calculated using Abbott's formula (Abbott 1925).

$$\textbf{\textit{Percenatageofmortality}} = \frac{Numberofdeadlarvae}{Numberoflarvaeintroduced} \text{x} 100$$

The median lethal concentrations LC_{50} and LC_{90} were calculated using the probit analysis method (Finney 1971).

Photocatalytic activity of CuONPs

The photocatalytic activity of the CuONPs was performed using the degradation of toxic dyes, viz., crystal violet and methylene blue (Sathiyavimal et al. 2018). Briefly, 10 mg of CuONPs was added with 100 mL of crystal violet or methylene blue dye (10 mg/L). Without CuONPs served as control. The mixture was appropriately stirred by a magnetic stirrer for 30 min and then kept in direct sunlight irradiation. At specific intervals, the samples were centrifuged at 10,000 rpm for 10 min, and the optical density was measured using a UV spectrophotometer. The following formula calculated the percentage of degradation efficiency (E).

$$E = \frac{C_0 - C_t}{C_0} \text{x } 100$$

where C_0 = the absorbance before treatment and Ct = the absorbance at the time.

Statistical analysis

Experiments were run in triplicates. The values are given as mean ± standard deviation. The tool used was Graphpad software (Instat and Prism 5.0 Demo version). The assay values were subjected to two-way ANOVA comprising Dunnet's multiple comparison tests. The mean difference is considered significant at the levels of $*p < 0.05$, $**p < 0.01$, and $***p < 0.001$. Statistical analyses of larvicidal bioassay were carried out with SPSS software (version 25).

Results and discussion

Biosynthesis and characterization of CuONPs

The work was devised to synthesize CuONPs using *R. cordifolia* for emancipating the eco-friendly method for wide application perspectives. The color change of the solution from light brown to brownish-black validated the green synthesis of CuONPs employing *R. cordifolia* extract (Fig. 1a). The development of color steadily increased with an increase in incubation time. After 150 min of incubation, the solution color remained stable, indicating the saturation of CuONPs synthesis (Fig. 1a). UV–Vis spectroscopy results showed a significant absorption between 250 and 300 nm, implying the generation of copper oxide nanoparticles. The surface plasma resonance (SPR) effect was responsible for changing in color, shape, and size of the nanoparticles (Sankar et al. 2014). These results are similar to that of bio-fabricated copper oxide nanoparticles wherein Andean blackberry fruit, *P. guajava* leaf extract, and *Carica papaya* showed the transition of excitation potentials revealing the biosynthesis (Sankar et al. 2014; Singh et al. 2019). Secondary metabolites produced by plants are essential for the reduction of harmful and stabilizing agents during the synthesis of metal oxide nanoparticles.

The FT-IR spectrum was employed to determine the bioactive components in the plant extract and to evaluate the functional group interaction of green synthesized CuONPs. The FT-IR spectra of biologically synthesized CuONPs are shown in Fig. 1b. The band at 3265 cm^{-1} corresponds to -OH stretch due to carboxylic acids. The peak obtained at 1648 cm^{-1} responds to –C = C– stretch due to alkenes. The peak observed at 1482, 1376, and 1802 cm^{-1} was attributed to the C-H, N–O, and C−N vibration modes of alkane, nitro, and aromatic compounds. The peak 894 cm^{-1} was ascribed to the C–H vibration due to alkene functional groups. The characteristic peaks at 631 cm^{-1} and 550 cm^{-1} could be attributed to the vibration mode of metal oxide (CuO) in the green synthesized CuONPs. Thus, FT-IR analysis validated the presence of carboxylic acids, alkenes, esters, alcohols, and aromatic nitro compounds in the green synthesized CuONPs. The abundance of such bioactive plant secondary metabolites may have resulted in the reduction and encapsulation of CuONPs. These findings corroborated an earlier study on the biosynthesis of CuONPs from plant materials (Sathiyavimal et al. 2018, 2021).

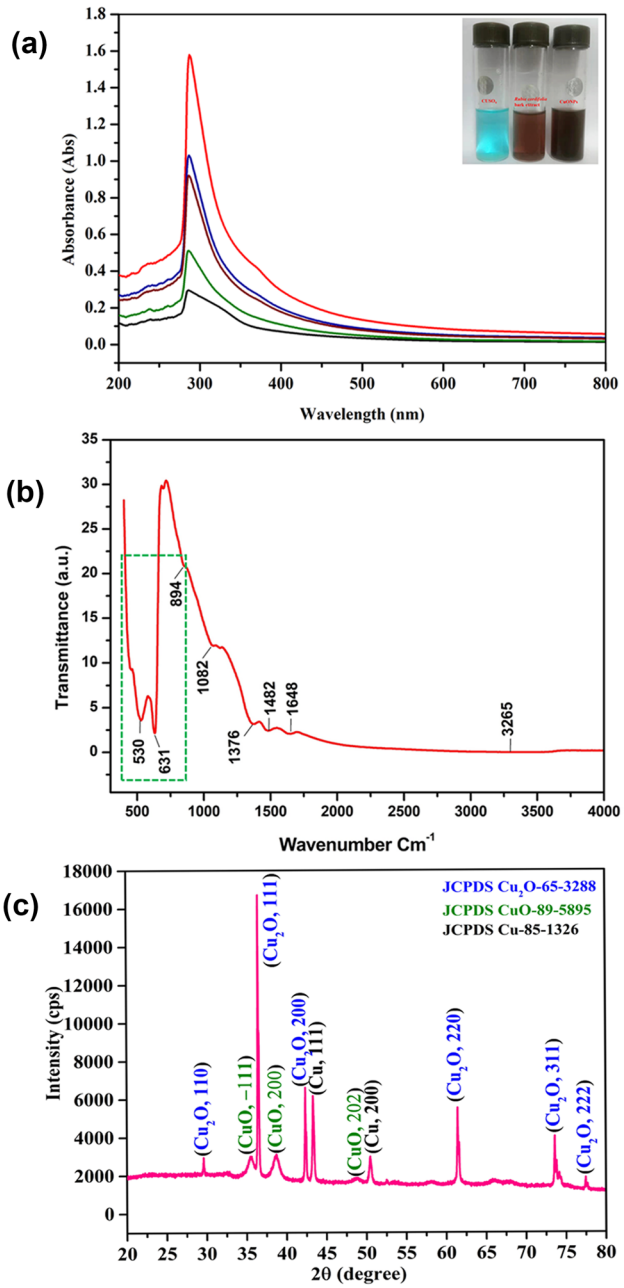

Fig. 1 Characterization **of** *Rubia cordifolia* CuONPs. **(a)** Ultraviolet–visible spectrum, **(b)** Fourier transform infrared spectrum, and **(c)** X-ray powder diffraction pattern

The XRD spectra of green biosynthesized CuONPs revealed a range of diffraction patterns at 29.63°, 35.57°, 36.50°, 38.96°, 42.40°, 43.32°, 48.82°, 50.45°, 61.52°, 73.69°, and 77.56°, corresponding to the (110), (− 111), (111), (200), (200), (111), (− 202), (200), (220), (311), and (222), respectively. The prepared sample shows the presence of mixed crystalline phases of cubic copper (Cu), monoclinic cupric oxide (CuO), and cubic cuprous oxides (Cu_2O) (Fig. 1c). Among the three-phase indices, Cu and Cu_2O show a highly symmetric cubic phase, while CuO reveals a low-symmetric monoclinic structure. Hence, the Cu and Cu_2O phase generation is majorly found in the prepared material. The XRD result of CuONPs has significantly matched with JCPDS file no 85–1326 (Cu), 89–5895 (CuO), and 65–3288 (Cu_2O), respectively. The standpoints of the strong peaks are entirely consistent with the monoclinic structure. The X-ray diffraction analysis revealed that the synthesized copper oxide nanoparticles are crystalline in nature. This result agrees with similar findings indicated as monoclinic cubic structure (Al-Saeedi et al. 2021; Sathiyavimal et al. 2021).

The surface shape and size of the CuONPs were examined using FE-SEM, and energy dispersive X-ray analysis (EDX) analysis revealed the existence of the elements in CuONPs. The *R. cordifolia* extracts mediated CuONPs demonstrate rough agglomerates and irregular spherical shapes (Fig. 2a). EDX analysis confirmed the maximum proportions of elemental copper (Cu) and oxide (O) peaks were found in CuONPs (Fig. 2b). These findings corroborated earlier research observations on CuONPs nanoparticles from *Psidium guajava* leaf extract (Singh et al. 2019).

The determination of normal particle size and surface charge of nanoparticles were studied using DLS analysis. Figure 2(c) reveals that the average particle size distribution of *R. cordifolia* green synthesized copper oxide nanoparticles was 50.72 nm which was comparable size (50 nm) of CuONPs synthesized using *Sida acuta* extract (Sathiyavimal et al. 2018). The zeta potential distribution revealed a negative value of about − 11.2 mV (Fig. 2d). It was indicated that the size and charge distribution of the synthesized nanoparticles facilitated or improved CuONPs' biological properties. The larger adverse zeta potential demonstrated a high repulsive force between the nanoparticles, resulting in an intensification or augmentation of consistency. Similar, comparable negative zeta potential value was obtained in the biologically synthesized CuONPs from *Ruellia tuberosa* extract (Vasantharaj et al. 2019).

Antibacterial activity of CuONPs

Antibacterial activities were precisely grouped to assess a couple of Gram-negative and Gram-positive pathogens. The four representative bacterial pathogens, *E. coli* MTCC 1610, *P. aeruginosa* MTCC 1953, and *S. aureus* MTCC 96, and *B. cereus*, showed the zone of inhibition at 500 µg/mL concentrations (Table 1). However, the increased inhibitory profiles were found at 400 µg/mL and not for 100, 200, and 300 µg/mL concentrations. The inhibitory zone of CuONPs (500 µg/mL) observed for tested pathogenic bacteria is 7 mm for *E. coli* MTCC 1610; 14 mm for *P. aeruginosa* MTCC 1953; 11 mm for *S. aureus* MTCC 96; and 6 mm for *Bacillus cereus.* Hence, it can be ascertained that an increase in concentrations will have optimal outcomes for effective antibacterial activity. SEM analysis revealed that the CuONPs would rupture the *P. aeruginosa* MTCC 1953 and *S. aureus* MTCC 96 bacterial cell wall and cause membrane damage at a maximum concentration (500 µg/mL), thus, leading to the death of bacteria (Fig. 3). On the contrary, the rare medicinal plant *Cissus arnotiana* showed activity against *E. coli* at 75 µg/mL using copper nanoparticles. These results can be corroborated by the usage of rare plant and a single bacterial species, whereas the present assessment indicated the utility of four bacterial species (Rajeshkumar et al. 2019). *Citrus limon* derived copper nanoparticles have been proved to possess similar antibacterial properties, showing cost-effectiveness and eco-friendly nature (Amer and Awwad 2021). Similar results were also witnessed in the synthesis of green copper nanoparticles against the same bacterial pathogens employed in the present study (Murthy et al. 2020). Nevertheless, the *R. cordifolia* CuONPs have coercive antibacterial properties, and antioxidant capabilities indicate the further drug design and reduced toxicity levels. CuONPs synthesized from citron juice (*Citrus medica* Linn.) showed potential antibacterial and antifungal potentials and were specifically suitable for plant pathology applications against *Fusarium wilt* (Shende et al. 2015). Some research studies on copper nanoparticles have revealed that the noxiousness of copper ions would lead to rapid DNA degradation and decrease bacterial respiration. Further, in certain Gram-negative bacteria, copper ions may amend the conformation and electron transferase of the associated reductase leading to the suppression of cytochromes in the membrane (Warnes and Keevil 2011). Thus, the versatile applications of the CuONPs synthesized using *R. cordifolia* can have both environmental and biomedical applications. However, field trials and randomized controlled clinical trials are necessitated for essential applications. Ample reports have proved the antibacterial efficacies of copper nanoparticles synthesized from plant extracts.

Antioxidant activity of CuONPs

The in vitro antioxidant profiles of CuONPs are reported cohesively based on reducing power, DPPH, ABTs, and nitric oxide scavenging assays. Results indicated that the quenching of DPPH free radicals by CuONPs significantly increased with an increasing concentration from 10–100 µg/

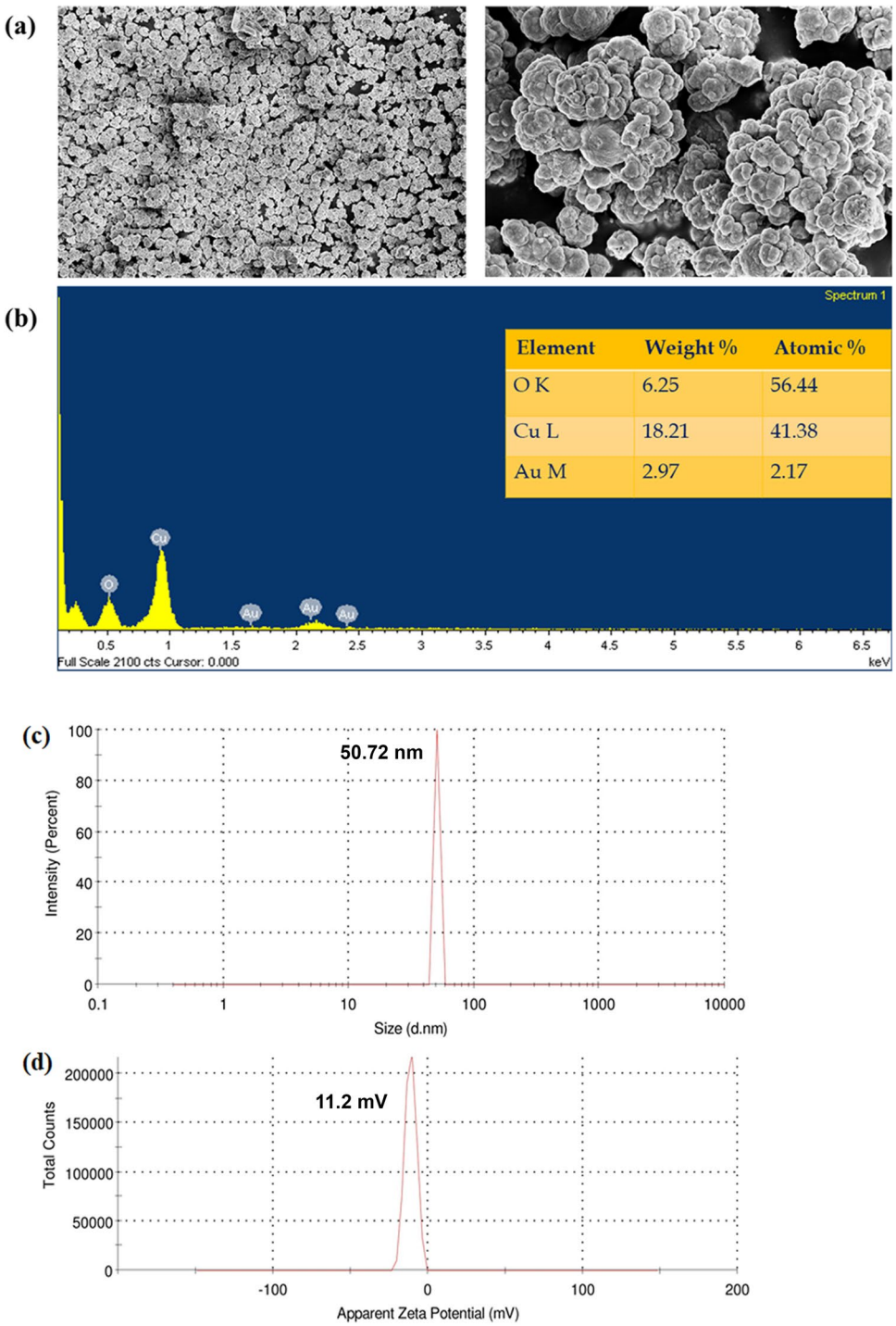

Fig. 2 **a** Field emission scanning electron microscopy images of *Rubia cordifolia* CuONPs. **(b)** EDX pattern of CuONPs. **(c)** Dynamic light scattering analysis of particle size distribution. **(d)** Zeta potential value of CuONPs

mL. The DPPH quenching ability of CuONPs exhibited 60.74% at 100 µg/mL concentration which is significantly ($p < 0.05$) lesser than the reference standard L-ascorbic acid (88.76%) (Fig. 4a). Furthermore, CuONPs exhibit the ABTS quenching activity of about 70.88% at the maximum dose of 100 µg/mL, which is considerably lesser than L-ascorbic acid (92.82%) (Fig. 4b). The CuONPs have exhibited better nitric acid scavenging activity in a dose-dependent way with the maximum activity of 65.46% at 100 µg/mL, which was less compared to the standard L-ascorbic acid (82.42%) (Fig. 4c). The maximum scavenging of reducing power by CuONPs was 71.44% at 100 µg/mL concentration in a dose-dependent manner (Fig. 4d). The CuONPs from endophytic fungi could scavenge free radicals at low concentrations, which were determined by DPPH, nitric oxide radical scavenging tests, and reducing power ability (Mani et al.

Table 1 Antibacterial activity of *R. cordifolia* CuONPs against bacterial pathogens

Sample concentration (µg/mL)	Zone of inhibition (mm)			
	Escherichia coli MTCC 1610	*Pseudomonas aeruginosa* MTCC 1934	*Staphylococcus aureus* MTCC 96	*Bacillus cereus*
100	3	5	2	NE
200	5	8	5	NE
300	6	9	8	NE
400	6	11	10	4
500	7	14	11	6

NE no effect detected

2021). *Magnolia kobus* leaf extracts were proved for better eco-friendly attributes than silver nanoparticles against *E. coli*, showing the significance of copper nanoparticles (Lee et al. 2013). The antioxidant activities of the leaf extracts of *Eclipta prostrata* derived copper nanoparticles were proved effective in in vitro anticancer activities against HepG2 cell lines showing hepatotoxicity (Chung et al. 2017). Hence, the present extensive antioxidant profiling will potentially effectuate anticancer activities against major cancers. CuONPs have been attributed to linking reactive oxygen species for effective antibacterial potentials (Gopinath et al. 2016). Moreover, it has also been proved that leaf extracts derived from copper oxide nanoparticles from *Allium sativum* and *Allium eriophyllum* Boiss possess subsequent antibacterial and antioxidant potentials (Velsankar et al. 2020; Zhao et al. 2020). Thus the coherent assessment of both properties will have potential implications and positive outcomes. Hence, the present analysis will aid in further research for assessing the antibacterial, antifungal, and anticancer activities using CuONPs. By and large, the CuONPs showed promising free radical scavenging to improve immune function against oxidative damage.

Larvicidal bioassay of CuONPs

The results obtained from the larvicidal bioassay clearly indicate that a significant larvicidal effect on *Aedes*, *Culex*, and *Anopheles* was exerted by the green synthesized CuONPs. Further, LC_{50} values of 26.88 ppm, 16.93 ppm, and 26.60 ppm were recorded against *Aedes aegypti*, *Anopheles stephensi*, and *Culex quinquefasciatus*, respectively. The larvicidal activity of the CuONPs were found to be dose-dependent manner. CuONPs at 10 ppm concentration showed 35, 43, and 31% of mortality against *A. aegypti*, *A. stephensi*, and *C. quinquefasciatus*. An increase in the concentration of CuONPs to 50 ppm exhibited a high percentage of larval mortality (65, 80, and 72%), respectively, for *A. aegypti*, *A. stephensi*, and *C. quinquefasciatus* (Table 2). Microbial extract (*Metarhizium robertsii*) mediated CuONPs exhibited 80, 94, and 100% mortality in *A. aegypti*, *A. stephensi*, and *C. quinquefasciatus*, respectively, at 25 µg/mL concentration with the LC_{50} value of 7.796, 3.478, and 3.136 µg/mL. However, the present study recorded higher LC_{50} values, and the difference in the larvicidal effect might be due to the difference in bioactive compounds in fungal and plant extracts (Vivekanandhan et al. 2021). Mosquito

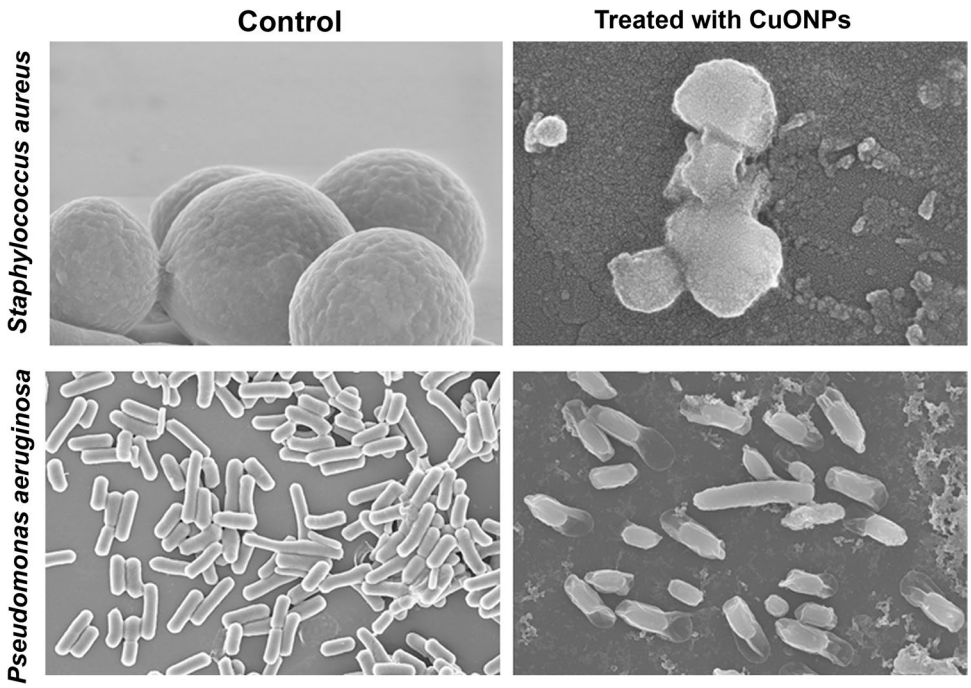

Fig. 3 FE-SEM images showed normal and damaged cells of bacterial pathogens treated with CuONPs showing cell damages

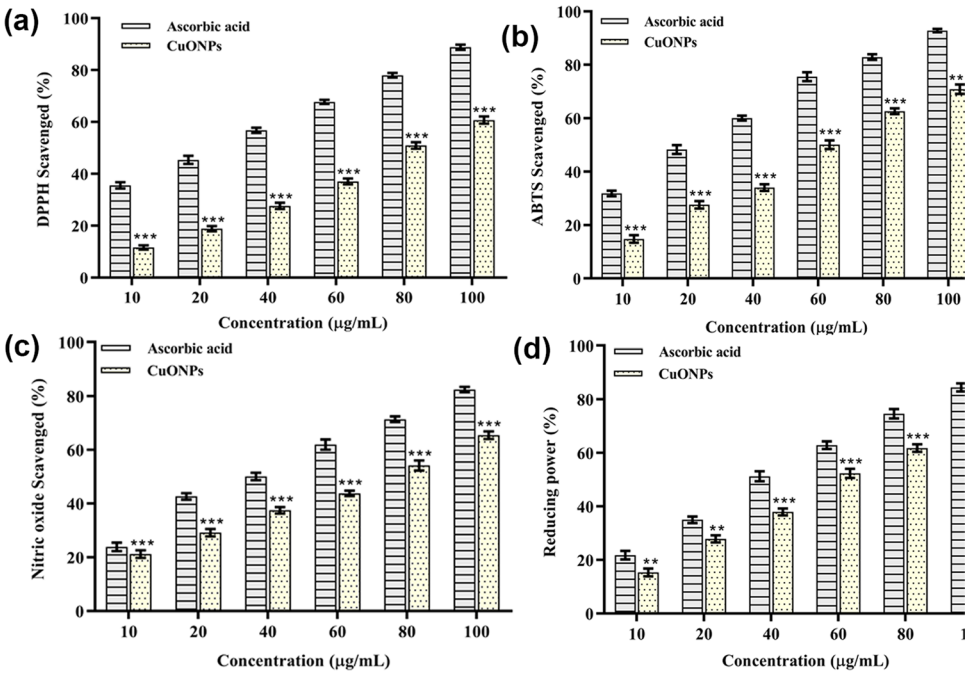

Fig. 4 Antioxidant activity of *Rubia cordifolia* CuONPs. **(a)** DPPH scavenging. **(b)** ABTs radical scavenging. **(c)** Nitric oxide scavenging. **(d)** Reducing power capacity. The mean difference is considered significant at the levels of $*p < 0.05$, $**p < 0.01$, and $***p < 0.001$

Table 2 Acute toxicity of synthesized copper nanoparticles against larvae of three mosquito species

Mosquito	Concentration (ppm)	Mortality (%)	LC_{50} (ppm) (LCL-UCL)	LC_{90} (ppm) (LCL-UCL)	χ^2 (df = 3)	Regression equation
Aedes aegypti	10	35 ± 3.54	26.88 (19.18–33.17)	97.45 (76.28–50.53)	0.930	$X = 0.02$ $Y = -0.49$
	20	48 ± 7.58				
	30	54 ± 8.94				
	40	59 ± 6.52				
	50	65 ± 8.66				
Anopheles stephensi	10	43 ± 5.70	16.93 (8.86–22.05)	68.51 (57.84–89.02)	1.416	$X = 0.02$ $Y = -0.42$
	20	56 ± 6.52				
	30	58 ± 7.58				
	40	73 ± 8.37				
	50	80 ± 13.69				
Culex quinquefasciatus	10	31 ± 8.94	26.60 (21.72–30.84)	74.62 (63.49–94.93)	0.528	$X = 0.03$ $Y = -0.71$
	20	44 ± 6.52				
	30	56 ± 7.42				
	40	64 ± 9.62				
	50	72 ± 13.04				

LC_{50} = lethal concentration that kills 50% of the exposed organisms

LC_{90} = lethal concentration that kills 90% of the exposed organisms

LCL = lower confidence limit

UCL = upper confidence limit

χ^2 = chi-square value

d.f. = degrees of freedom

larvae feed on sterols from plant decays, and the possible cause of mortality among mosquito species due to CuONPs might be attributed to inhibition of sterol carrier proteins-2 (SCP-2). The phytosterols are converted into a cholesterol which plays a significant role in developing cell membrane and growth of the larvae. SCP-2 are also involved in the transfer of cholesterol to mitochondria. Hence, the inhibition of SCP-2 effectively inhibits the growth of mosquito larvae

(Angajala et al. 2018). A recent study demonstrated that the CuONPs via *Allium sativum* extract had noticeable larvicidal efficacy against *Anopheles subpictus* mosquito larvae (Velsankar et al. 2020).

Photocatalytic activity of CuONPs

R. cordifolia CuONPs against methylene blue and crystal violet dye under sunlight irradiation showed escalated degradation ability ranging from 0 to 6-h incubation (Fig. 5a and 5b). The effective degradation efficacy of methylene blue (81.84%) and crystal violet (64.0%) dye using CuONPs shows the potential application in environmental impact management of pollution abatement. Similar green synthesis of CuONPs derived from the plant extracts of *Celastrus paniculatus* showed photocatalysis and antifungal properties. Photocatalytic activity of *Sida acuta*-mediated CuONPs showed considerable dye degradation ability for methylene blue (93%) and crystal violet (87%) dye at 150 min

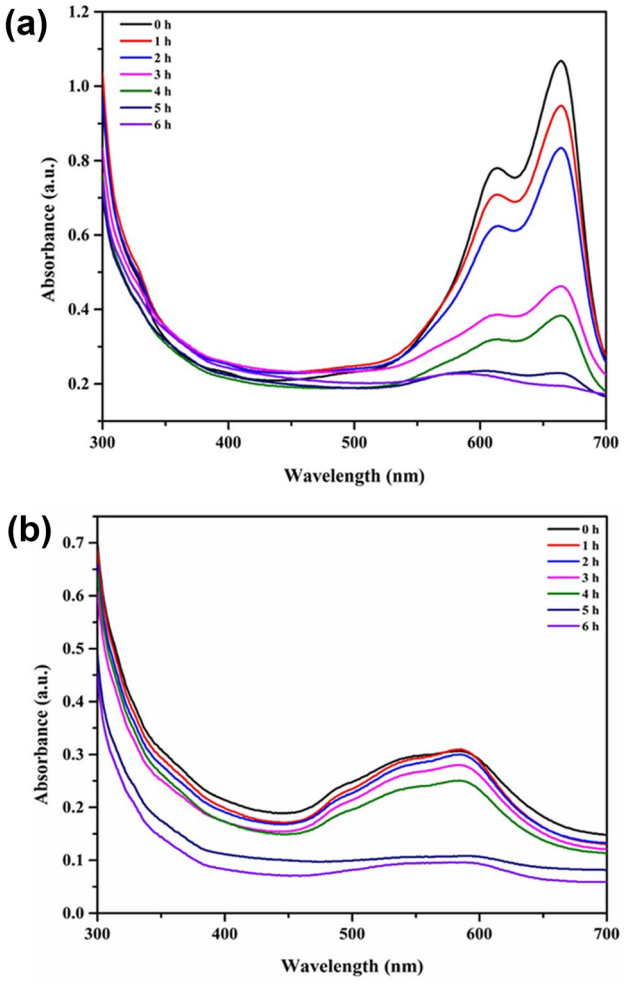

Fig. 5 Photocatalytic activity of *Rubia cordifolia* CuONPs against **(a)** methylene blue and **(b)** crystal violet dye under sun light irradiation

(Sathiyavimal et al. 2018). These findings demonstrate the multifaceted applications of green synthesis that are both cost-effective and environmentally acceptable (Mali et al. 2020). In a similar study, the biodegradation potentials of the leaf extracts of *Euphorbia esula* L. have been proved effective for 4-nitrophenol reduction (Nasrollahzadeh et al. 2014). Methylene blue removal for toxic pollutants removal employing *Cynomorium coccineum* copper nanoparticles has been proved effectively based on adsorption interaction (Sebeia et al. 2020). Ample research concerning photocatalytic profiles of plant-mediated biotransformation and intricate chemical reactions for successful degradation of dyes has been documented. As the plant utilized in the study is largely studied earlier for dye degradation, the present preliminary assessment corroborates to a holistic perception of the utility of CuONPs for versatility of antibacterial and antioxidant properties. The future prospects for the effectuating benefits in using the nanomedicine for combating major cancers and the intrinsic foundations are thus implicated.

The present study accounts for the first report of CuONPs synthesized using *R. cordifolia*. The plant represents as a component for traditional Chinese medicine and Ayurvedic principles. The applications of the plant in dye degradation and biomedical pharmaceutics have been amply reported. Nevertheless, the molecular dissection of the mechanistic action mode remains intricately studied for improvising wide applications. Alleviating the symptoms of the disease and environmental-friendly bioremediation strategies will have potential applications in nanophytomedicine and ecological significance. However, nanoencapsulation and facile synthesis have been explicitly addressed in large-scale human welfare applications. This preliminary characterization will be a blueprint for invigorating the pivotal roles for nanotechnology, plant physiology, metabolism, and versatile applications.

Conclusions and future prospects

CuONPs were synthesized and characterized using *R. cordifolia.* The characteristics of the nanoparticles were affirmed using standard methodologies for demarcating the intricate parameters of nano-basis. The UV–Vis spectrophotometer, FT-IR spectrum, XRD analysis, FE-SEM images, DLS, and zeta potential show the appropriate characteristics of the biosynthesis. The absorbance peak between 250 and 300 nm clearly demonstrates the formation of CuONPs in the UV–visible spectrum. FT-IR spectroscopy results showed the presence of bioactive functional groups essential for copper ion reduction. FE-SEM and DLS analysis revealed that the eco-friendly synthesized CuONPs are spherical-shaped with a mean particle size of 50.72 nm. Additionally, the zeta potential demonstrates its robustness at 11.2 mV. X-ray diffraction spectra

showed monoclinic cubic crystalline in nature. Antibacterial and antioxidant potentials are corroborated for a linking based on previous research. Nevertheless, a plethora of research is necessitated for coercing the antibacterial and antioxidant profiles. The antioxidant properties have been addressed for quenching the toxic metabolites based on ROS production using DPPH radical scavenging, nitric oxide scavenging, and reducing power assays. The present assessment proves an effective launchpad for further research on specific cancers like hepatocellular carcinoma induced by *Helicobacter pylori* infections. Additionally, maximum concentration (50 ppm) of CuONPS mediated by *R. cordifolia* bark extract revealed a considerable percentage of larval mortality against *A. aegypti* (65%), *A. stephensi* (80%), and *C. quinquefasciatus* (72%). Further, the conventional usage of the plant in dye degradation has been addressed to photocatalysis and the redox potentials that aid in the research perspectives for protein interactions and metabolic crosstalk. Thus, nanomedicine employing plant materials like *R. cordifolia* can be addressed to decipher the protein interaction network with regulatory prospects for addressing the optimal benefits. Transcriptomic, metabolomic, RNAome studies, culturomics, and big data analytics will have significant molecular prospects. Hence, the linking possibilities for photocatalytic and antibacterial activities and molecular dissection will provide an additional scenarios of research. Future research regarding patenting nano encapsulated plant extracts, environmental trials, and commercialization will gain momentum as the rise in pollution due to escalating population.

Acknowledgements The first author (A.V) is thankful for the Award of UGC-RGN Fellowship, Govt. of India and Postdoctoral Researcher at Jiangsu University, PR, China. The authors (A.V and Y.M) acknowledge the"Foreign Scientist Talented Project"awarded by the Ministry of Science and Technology, China.

Author contribution **A. Vinothkanna:** Conceptualization, Methodology, Formal analysis, Validation, Visualization, Writing-original draft. **K. Mathivanan:** Formal analysis and validation. **S. Ananth:** Formal analysis and validation **Y. Ma:** Project administration, Validation, Visualization, Writing-review and editing. **S. Sekar:** Conceptualization, Supervision, Project administration, Funding acquisition, Writing-review and editing.

Data Availability All data generated and analyzed during this study are included in this article.

Declarations

Ethics approval Not applicable.

Consent to participate Not applicable.

Consent for publication Not applicable.

Competing interests The authors declare no competing interests.

References

Abbott WS (1925) A method of computing the effectiveness of an insecticide. J Econ Entomol 18:265–267

Al-Saeedi SI, Al-Senani GM, Abd-Elkader OH, Deraz NM (2021) One pot synthesis, surface and magnetic properties of Cu_2O/Cu and Cu_2O/CuO nanocomposites. Curr Comput-Aided Drug Des 11:751

Amer M, Awwad A (2021) Green synthesis of copper nanoparticles by Citrus limon fruits extract, characterization and antibacterial activity. Chem Int 7:1–8

Angajala G, Pavan P, Subashini R (2018) One-step cost effective biofabrication of copper nanoparticles from *Aegle marmelos* correa aqueous leaf extract and evaluation of its anti-inflammatory and mosquito larvicidal efficacy. Biocatal Agric Biotechnol 16:586–593

Burlacu E, Tanase C (2021) Anticancer Potential of natural bark products—a review. Plants 10:1895

Chen X-Q, Li Z-H, Liu L-L, Wang H, Yang S-H, Zhang J-S, Zhang Y (2021) Green extraction using deep eutectic solvents and antioxidant activities of flavonoids from two fruits of *Rubia* species. LWT - Food Sci Technol 148:111708

Chung IM, Abdul Rahuman A, Marimuthu S, Vishnu Kirthi A, Anbarasan K, Padmini P, Rajakumar G (2017) Green synthesis of copper nanoparticles using *Eclipta prostrata* leaves extract and their antioxidant and cytotoxic activities. Exp Ther Med 14:18–24

Deshkar N, Tilloo S, Pande V (2008) A comprehensive review of *Rubia cordifolia* Linn. Pharmacogn Rev 2:124

Finney D (1971) Probit analysis method, 2nd edn. Press, Camp. Uni

Gleba M, VandenBerghe I, Aldenderfer M (2016) Textile technology in Nepal in the 5th-7th centuries CE: the case of Samdzong. STAR: Science Technology of Archaeological Research 2:25–35

Gong X-P, Sun Y-Y, Chen W, Guo X, Guan J-K, Li D-Y, Du G (2017) Anti-diarrheal and anti-inflammatory activities of aqueous extract of the aerial part of *Rubia cordifolia*. BMC Complement Altern Med 17:1–9

Gopinath V, Priyadarshini S, Al-Maleki A, Alagiri M, Yahya R, Saravanan S, Vadivelu J (2016) In vitro toxicity, apoptosis and antimicrobial effects of phyto-mediated copper oxide nanoparticles. RSC Adv 6:110986–110995

Hu Y-y, Zhang X-j, Zhang Z-h, Wang Z, Tan N-h (2020) Qualitative and quantitative analyses of quinones in multi-origin Rubia species by ultra-performance liquid chromatography-tandem mass spectrometry combined with chemometrics. J Pharm Biomed Anal 189:113471

Lee HJ, Song JY, Kim BS (2013) Biological synthesis of copper nanoparticles using *Magnolia kobus* leaf extract and their antibacterial activity. J Chem Technol Biotechnol 88:1971–1977

Mali SC, Dhaka A, Githala CK, Trivedi R (2020) Green synthesis of copper nanoparticles using *Celastrus paniculatus* Willd. leaf extract and their photocatalytic and antifungal properties. Biotechnol. Rep. 27:e00518

Mani VM, Kalaivani S, Sabarathinam S, Vasuki M, Soundari AJPG, Das MA, Elfasakhany A, Pugazhendhi A (2021) Copper oxide nanoparticles synthesized from an endophytic fungus *Aspergillus terreus*: Bioactivity and anti-cancer evaluations. Environ Res 201:111502

Mariswamy SD, Thimmaiah CK, Basappachidananda VK, Basavaraju M, Arkeswaraiah CN (2021) Antimicrobial, haemolytic and antibiofilm assay of green synthesized silver nanoparticles by aqueous extracts of *Rubia cordifolia*. Int J Pharm Sci Rev Res 28:174–184

Meena V (2015) Manjistha (*Rubia cordifolia*)-a helping herb in cure of acne. Journal of Ayurveda Holistic Medicine 3:11–17

Murthy H, Desalegn T, Kassa M, Abebe B, Assefa T (2020) Synthesis of green copper nanoparticles using medicinal plant *Hagenia*

abyssinica (Brace) JF. Gmel. leaf extract: Antimicrobial properties. J Nanomater 2020:1–12

Nasrollahzadeh M, Sajadi SM, Khalaj M (2014) Green synthesis of copper nanoparticles using aqueous extract of the leaves of *Euphorbia esula* L and their catalytic activity for ligand-free Ullmann-coupling reaction and reduction of 4-nitrophenol. RSC Adv 4:47313–47318

Negi DS (2018) Antioxidant and Photocatalytic activity of green synthesized zinc oxide nanoparticles using stem extract of *Rubia cordifolia*. International Journal of Engineering, Science and Mathematics 7:402–412

Rajeshkumar S, Menon S, Kumar SV, Tambuwala MM, Bakshi HA, Mehta M, Satija S, Gupta G, Chellappan DK, Thangavelu L (2019) Antibacterial and antioxidant potential of biosynthesized copper nanoparticles mediated through *Cissus arnotiana* plant extract. J Photochem Photobiol B: Biol 197:111531

Sankar R, Maheswari R, Karthik S, Shivashangari KS, Ravikumar V (2014) Anticancer activity of *Ficus religiosa* engineered copper oxide nanoparticles. Mater Sci Eng C 44:234–239

Sarwar N, Humayoun UB, Kumar M, Zaidi SFA, Yoo JH, Ali N, Jeong DI, Lee JH, Yoon DH (2021) Citric acid mediated green synthesis of copper nanoparticles using cinnamon bark extract and its multifaceted applications. J Clean Prod 292:125974

Sathiyavimal S, Vasantharaj S, Bharathi D, Saravanan M, Manikandan E, Kumar SS, Pugazhendhi A (2018) Biogenesis of copper oxide nanoparticles (CuONPs) using *Sida acuta* and their incorporation over cotton fabrics to prevent the pathogenicity of Gram negative and Gram positive bacteria. J Photochem Photobiol B: Biol 188:126–134

Sathiyavimal S, Vasantharaj S, Veeramani V, Saravanan M, Rajalakshmi G, Kaliannan T, Al-Misned FA, Pugazhendhi A (2021) Green chemistry route of biosynthesized copper oxide nanoparticles using *Psidium guajava* leaf extract and their antibacterial activity and effective removal of industrial dyes. J Environ Chem Eng 9:105033

Sebeia N, Jabli M, Ghith A, Saleh TA (2020) Eco-friendly synthesis of *Cynomorium coccineum* extract for controlled production of copper nanoparticles for sorption of methylene blue dye. Arab J Chem 13:4263–4274

Sekar S, Mariappan S (2010) Fermented medicines of Ayurveda: a treatise. LAP LAMBERT Academic Publishing, Germany

Shende S, Ingle AP, Gade A, Rai M (2015) Green synthesis of copper nanoparticles by *Citrus medica* Linn. (Idilimbu) juice and its antimicrobial activity. World J Microbiol Biotechnol 31:865–873

Singh J, Kumar V, Kim K-H, Rawat M (2019) Biogenic synthesis of copper oxide nanoparticles using plant extract and its prodigious potential for photocatalytic degradation of dyes. Environ Res 177:108569

Vasantharaj S, Sathiyavimal S, Saravanan M, Senthilkumar P, Gnanasekaran K, Shanmugavel M, Manikandan E, Pugazhendhi A (2019) Synthesis of ecofriendly copper oxide nanoparticles for fabrication over textile fabrics: characterization of antibacterial activity and dye degradation potential. J Photochem Photobiol B: Biol 191:143–149

Velsankar K, RM AK, Preethi R, Muthulakshmi V, Sudhahar S (2020) Green synthesis of CuO nanoparticles via *Allium sativum* extract and its characterizations on antimicrobial, antioxidant, antilarvicidal activities. J Environ Chem Eng 8:104123

Vinotha V, Yazhiniprabha M, Raj DS, Mahboob S, Al-Ghanim KA, Al-Misned F, Govindarajan M, Vaseeharan B (2020) Biogenic synthesis of aromatic cardamom-wrapped zinc oxide nanoparticles and their potential antibacterial and mosquito larvicidal activity: An effective eco-friendly approach. J Environ Chem Eng 8:104466

Vinothkanna A, Sekar S (2018) Antioxidant activity of fermented traditional medicines of Indian Ayurveda-*Ashokarishta*, *Aswagandharishta* and *Dasamoolarishta*. Biosci Biotechnol Res Asia 15:699–709

Vivekanandhan P, Swathy K, Thomas A, Kweka EJ, Rahman A, Pittarate S, Krutmuang P (2021) Insecticidal efficacy of microbial-mediated synthesized copper nano-pesticide against insect pests and non-target organisms. Int J Environ Res Public Health 18:10536

Warnes S, Keevil C (2011) Mechanism of copper surface toxicity in vancomycin-resistant enterococci following wet or dry surface contact. Appl Environ Microbiol 77:6049–6059

Yugandhar P, Vasavi T, Devi PUM, Savithramma N (2017) Bioinspired green synthesis of copper oxide nanoparticles from *Syzygium alternifolium* (Wt.) Walp: characterization and evaluation of its synergistic antimicrobial and anticancer activity. Appl Nanosci 7:417–427

Yusuf M, Shahid M, Khan MI, Khan SA, Khan MA, Mohammad F (2015) Dyeing studies with henna and madder: a research on effect of tin (II) chloride mordant. J Saudi Chem Soc 19:64–72

Yusuf M, Mohammad F, Shabbir M (2017) Eco-friendly and effective dyeing of wool with anthraquinone colorants extracted from *Rubia cordifolia* roots: optimization, colorimetric and fastness assay. J King Saud Univ Sci 29:137–144

Zhao H, Su H, Ahmeda A, Sun Y, Li Z, Zangeneh MM, Nowrozi M, Zangeneh A, Moradi R (2020) Biosynthesis of copper nanoparticles using *Allium eriophyllum* Boiss leaf aqueous extract; characterization and analysis of their antimicrobial and cutaneous wound-healing potentials. Appl Organomet Chem 34:e5587